Maximizing Firm Wind Connection to Security Constrained Transmission Networks

Daniel J. Burke, *Graduate Student Member, IEEE*, and Mark J. O'Malley, *Fellow, IEEE*

***Abstract*—Prudent use of existing transmission capacity could be achieved by an optimal allocation of wind capacity to distinct transmission nodes. The statistical interdependency of geographically separate wind sites and the partially-dispatchable nature of wind power require a collective analysis of all potential wind farms over an extended time-frame in any optimized transmission planning study. The methodology presented in this paper separates this large optimization problem into smaller subtasks, including a year-long sequential time series hourly integer unit commitment, a linear dc load-flow network model with hourly security constraints, and a linear programming optimization model to estimate the maximum firm wind energy penetration for a given network. A novel maximal-vector based constraint redundancy analysis is employed to significantly reduce the linear programming optimization dimensionality. Firm wind capacity connections are facilitated in this paper—i.e., those to which wind curtailment to manage congestion is not applicable within a typical system "planning" timeframe analysis. Each bus is allocated firm capacity on the basis of maximizing the possible firm wind energy penetration in the transmission system as a whole, while preserving traditional network security standards.**

***Index Terms*—Computational geometry, linear programming redundancy, power transmission, wind energy.**

Nomenclature and Units

A. Indices

d	Linear constraint coefficient position index.
h	Time series hourly position index.
i	Network bus position index.
j	Network branch index.
k	Potential wind farm network location index.
r	DC load flow reference bus position index.
s	Power flow contingency scenario index.
v	Maximal-vector redundancy stop-criterion set index.

B. Constants

α_{ijs}	DC load flow power transfer distribution factors for line "j" with respect to bus "i" under contingency scenario "s".
D_{AVG}	Average system power demand level (MW).
L_j	Thermal capacity for branch "j" (MW).
λ_k	Capacity factor of wind farm "k".
λ_{AVG}	Capacity factor of system averaged wind power time series.
G	Number of generation sites in the power system.
N	Number of network branches in the system.
S	Total number of contingency scenarios considered.
T	Length of the wind power time series (years).
V	Maximal vector redundancy analysis stop-criterion.
$\Delta\delta$	Discrete wind energy penetration target increment.

C. Time Series

t_{kh}	Nominal 1-MW wind power time series "k" in hour "h" (MW).
t_h^{AVG}	Average value of all the nominal 1-MW wind power time series in hour "h" (MW).
t_h^{APR}	Geographically smoothed total system wind power production value in hour "h" (MW).
γ_{jhs}	Partial load flow solution of load/conventional plant in branch "j", hour "h" under contingency scenario "s" (MW).

D. Variables

C_k	"k" wind capacity optimization variables (MW).
C^{APR}	Approximated system total wind capacity (MW).
f_j	Power flow in branch "j" (MW).

Manuscript received November 07, 2008; revised September 15, 2009. First published December 01, 2009; current version published April 21, 2010. This work was conducted in the Electricity Research Centre, University College Dublin, Ireland, which is supported by Airtricity, Bord Gais, Bord na Mona, Cylon Controls, the Commission for Energy Regulation, Eirgrid, ESB International, ESB Networks, ESB Powergen, Siemens, South Western Services, and Viridian. The work of D. J. Burke was supported by Sustainable Energy Ireland through a postgraduate research scholarship from the Irish Research Council for Science Engineering and Technology. Paper no. TPWRS-00914-2008.

The authors are with the School of Electrical, Electronic and Mechanical Engineering, University College Dublin, Dublin 4, Ireland (e-mail: daniel.burke@ucd.ie; mark.omalley@ucd.ie).

Digital Object Identifier 10.1109/TPWRS.2009.2033931

M	Minimal-cardinality maximal-vector subset size.
σ	Wind energy penetration target proportion.
ω_d	Linear constraint coefficient at position "d".

I. Introduction

DUE to its environmentally friendly and cost-predictable nature, wind power is widely recognized as a promising alternative electric power generation source at a time of uncertain fossil fuel costs and concern over the harmful effects of climate change [1]. Many countries are considering ambitious future wind energy penetration scenarios [2]. Significant lead-time and investment are associated with the transmission system expansion required to facilitate wind connection at sites distant from traditional load and generation centers however [3]. Furthermore, public acceptance of large scale new-build infrastructure is currently low [4]. In the short-term, maximum use of existing transmission system resources could be made by an optimal wind capacity allocation strategy.

In some power systems (e.g., Great Britain [5]), wind developers may request a "firm" connection offer for investment certainty reasons. A firm connection offer is generally given if a generator does not cause network overload subsequent to plausible system security contingencies. Firm connection feasibility study is usually considered as a "planning" timeframe problem. System re-dispatch of generation using "operational" timeframe techniques to manage congestion [6] is not considered in this context as this would impinge upon the firm status of other generators connected to the network, and the true bulk system reliability could be limited by transmission constraints. Firm connections are therefore suitable for transmission networks where system operators prefer to have little or no grid congestion. Large standalone conventional plant firm connection was traditionally assessed using heuristic techniques at deterministic "base-case" scenarios (e.g., incremental-transfer-capability studies at the winter-day-peak and/or the summer-night-valley [7]). Given that the worst-case-scenarios for distributed wind power related flows could conceivably occur at off-peak conditions, clearly a more extensive analysis is required. The statistical interdependence of geographically distinct wind sites, their fluctuating power output, and the large volume of connection applications mean that a collective analysis of all potential wind plant sites over an extended timeframe must be at the kernel of any optimization approach.

The advantage of transmission analysis carried out over a wider range of operating points is that the power flow worst-case-scenarios may be identified without any simplistic base-case assumptions. Some analytical power flow techniques have been reported in [8] and [9] modeling a greater variation in generation power injections and customer demand patterns. As discussed in [10] however, a multivariate statistical sampling approach is more accurate for wind-related power-flow studies given the elaborate nature of power system multidimensional statistical dependency distributions with high wind penetration. However a purely random "Monte Carlo" sampling technique such as in [11] cannot account for any inter-temporal power system dependencies. The capability of a year-long multivariate sequential time-series method to model the influence of increased wind power inter-temporal variability on system unit commitment (applying conventional generation parameters such as start-up times, minimum up- and down-times, etc.) was highlighted in [12].

Maintaining an integer unit-commitment solution, while including the large number of security constraints that accompany a year-long system load flow analysis, presents a significant dimensionality challenge to the optimal wind capacity placement problem. A simple approach to represent multi-period wind variations was implemented in [12], using a multidimensional "binning" technique to group (and thereby reduce) the number of relevant power flow scenarios—this did not incorporate network security contingencies however. Significant dimensionality reduction can be carried out by investigating the structure of the firm capacity optimization problem—if linearized load flow methods are used, then many of the power flow security constraints over the extended time series are redundant and can be removed by an efficient preprocessing scheme [13].

The approach of [13], with a defined optimization cost function to minimize a wind turbine infrastructure economic cost criterion (by choosing the best wind resource sites), assumed a specific wind energy penetration target was initially feasible using firm wind capacity connection. This would be unrealistic in most power systems with significant targets and present transmission limitations—instead this paper attempts to maximize the firm wind energy potential of the existing system in the short-term prior to transmission expansion in the long-term. To this end the approach of [13] is improved and extended, with incremental firm wind energy penetration targets applied from a lower initial level until a limit is reached when the optimization model becomes infeasible. Section II of this paper outlines the methodology in more detail.

II. Methodology

A. Optimization Methodology Overview

A flowchart of the overall methodology is given in steps in Fig. 1. It is assumed that the transmission network is initially uncongested (i.e., existing conventional plant also has firm connection status), and that the addition of new firm wind capacity should preserve this situation—i.e., generation curtailment due to network constraints is inapplicable. Year-long nodal load and nominal 1-MW multivariate wind power hourly production time series are available as inputs. A low firm wind energy penetration target is initially selected for investigation—if this level of firm wind energy integration is feasible (through optimized allocation of individual wind capacities), the target can be increased in small discrete steps until additional firm wind energy connection is not possible without system congestion. For each incremental energy target, the overall firm wind capacity allocation problem (incorporating linear wind capacity investment variables, hourly integer unit-commitment/dispatch variables and hourly security-constrained network limitations)

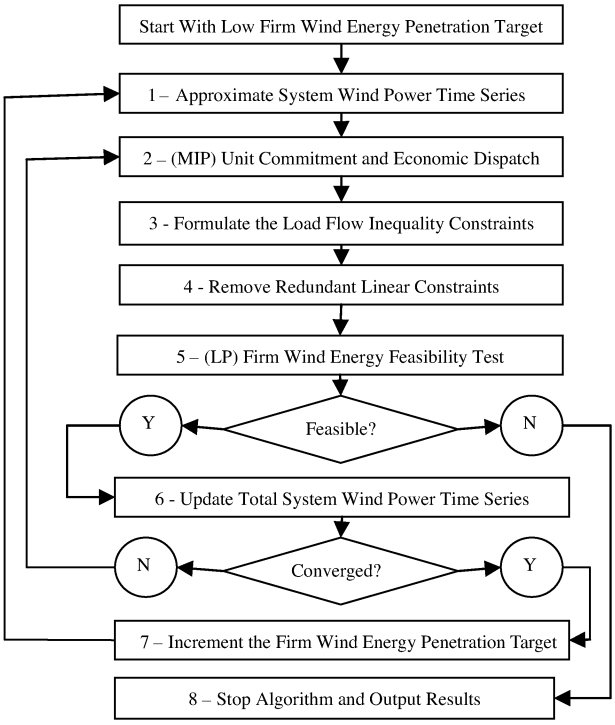

Fig. 1. Firm wind energy maximization methodology flowchart.

is separated into more tractable subproblems. An approximated total system wind time series facilitates the separation of the existing firm conventional plant mixed-integer scheduling task from a linear programming firm wind capacity allocation analysis. This problem decomposition into separate subtasks reduces the dimensionality and complexity of the overall firm capacity optimization problem, and allows an improved solution within practical computing capabilities. Given the separation of the individual subtasks, absolute global optimality cannot be guaranteed however.

The required approximate system-total wind power hourly production time series, (consistent with each incremental wind energy penetration target, and representing the system wind inter-hour variability pattern), can be generated using the multivariate nominal 1-MW wind power time series of the individual locations (step 1, Section II-B1). Using this initial wind power time series a sequential mixed-integer program (MIP) unit commitment and dispatch study is carried out to determine the MW outputs of existing firm conventional plant to serve the net load time series (step 2, Section II-B2)—this integer optimization does not require a network model as the system is initially assumed uncongested.

A dc load-flow network model subsequently uses this existing firm conventional plant hourly MW dispatch time series and the individual wind farm candidate locations' nominal 1-MW time series to define linear network security constraints from a set of critical line and generator contingency scenarios (step 3, Section II-B3). These linear constraints are formulated so that the power flows related to the optimized firm wind power capacities are "fitted-around" the power flows resulting from the firm conventional plant dispatch (step 2), while maintaining network security and power balance in each hour. The linear inequality constraints are subsequently preprocessed using a specifically tailored algorithm to remove any constraint redundancy over the extended timeframe of operation (step 4, Section II-B-4), and reduce the model size significantly with no compromise in accuracy [13].

The remaining nonredundant power flow linear constraints are integrated within a simple linear programming (LP) model to test the feasibility of this wind energy penetration target level with respect to the network capabilities (step 5, Section II-B5). The optimization variables are the individual wind capacity allocations to each candidate node. The resulting total system wind power output time series (as defined by the LP optimized wind capacities and their individual nominal 1-MW hourly time series) may not be precisely consistent with the system-wide approximate hourly input time series used to carry out the initial unit-commitment/dispatch of the firm conventional plant (step 6, Section II-B6). Steps 2–5 are therefore reiterated with this updated resultant system-total hourly time series as the input until power balance converges from one iteration to the next. If a converged solution is feasible, then the wind energy target can be incremented (step 7, Section II-B7) and the process repeated. On the other hand, if the LP model is deemed infeasible at any stage, the algorithm ends with the previous known feasible firm wind energy capacity allocation solution (step 8).

B. Optimization Methodology Subtasks

1) Approximating System Wind Power Output Time Series: A total system-wide wind power production time series is necessary to carry out the scheduling and dispatch of conventional plant. Simultaneous year-long nodal load and nominal 1-MW capacity wind power time series are available as inputs for each transmission network location, representing any geographic statistical and temporal multivariate dependencies independently of the wind plant capacity to be determined later. Each potential wind location (be it a single farm or a collection of local sites) will have its own capacity factor and individual variations in its nominal time series of power production. Therefore the total system wind power output time series required for the MIP conventional generation scheduling subtask (step 2) cannot be precisely defined prior to completing the individual wind plant capacity LP optimization subtask (step 5). However it can be initially assumed that the total system-wide wind power time series converges to a geographically-smoothened or approximate time series regardless of where the output wind power capacities are subsequently allocated. This is acceptable as within a power system of reasonable size and geographical wind capacity spread, the total wind power output is more influenced by the significant degree of interdependency contained in the collection of wind farm time series and the overall weather pattern in the wider geographical region, as opposed to any localized effects. Principle component analysis [14] or independent component analysis [15] can be carried out to study the interdependency present in the multiple wind power time series and substantiate this assumption.

In this paper, a simple hourly average of the multivariate nominal 1-MW wind power time series t_h^{AVG} was used to generate the initial system-wide hourly wind power output time series for the unit commitment stage of the first wind energy penetration

target level. An approximate turbine MW capacity C^{APR} required to serve a δ proportion of total yearly load energy demand by wind can be determined in (1) given the average system MW load of D^{AVG} and the average capacity factor of all the potential wind sites λ^{AVG} are known. The initial approximate hourly time series $\mathrm{t_h^{APR}}$ is determined by scaling the hourly average of the recorded nominal wind farm power time series $\mathrm{t_h^{AVG}}$ by C^{APR} as in (2). This wind power time series satisfies the annual wind energy penetration target δ while respecting system-wide inter-hourly wind variations, and is thus suitable for the initial unit-commitment and dispatch step:

$$\mathrm{C^{APR}} = \frac{\mathrm{D^{AVG}}}{\lambda^{\mathrm{AVG}}} \cdot \delta \tag{1}$$

$$\mathrm{t_h^{APR}} = C^{APR} \times t_h^{AVG}. \tag{2}$$

2) (MIP) Unit Commitment and Economic Dispatch: Connecting new wind generation will not only impact network flows by virtue of its own power injections, but also due to the consequential displacement of existing firm conventional plant in the overall power system operational context. Thus the multivariate interdependence of customer load, existing/new wind generation and existing conventional plant must be determined in conjunction with the task of finding the individual optimal firm wind capacity allocations. Increased wind penetration will lead to greater variability in the net power system load to which conventional plant must respond [16]. Investigating significantly increased wind capacity connection to transmission systems may therefore require an MIP scheduling model [12], with an accurate representation of the conventional plant inter-hourly constraints such as starting times, start costs, minimum up- and minimum down-times, ramp rate limits, etc. This may be of significant importance in power systems with inflexible conventional generation [17].

The geographically-smoothed time series of total wind power production $\mathrm{t_h^{APR}}$ from Section II-B1 can be subtracted from the total system load, and the resultant net system load time series input to a unit-commitment and dispatch model. This scheduling model can be applied in single-day or multi-day segments as required, with hourly integer resolution. Net system load variability effects over a typical year of operation are thus explicitly accounted for in this algorithm. Provision of primary reserve is included to respond to any single generation contingencies modeled in Section II-B3. The unit commitment and dispatch stage of this algorithm does not apply a network-constrained re-dispatch as it is assumed the firm connection status of generation already present in the system should be respected—i.e., it is assumed that the system is initially uncongested, and should remain so subsequent to the firm wind capacity addition. The output variables of this step are the least-cost MW power and reserve hourly dispatch of each firm conventional generator in the system for the given wind penetration level δ.

Stochastic unit-commitment of conventional plant accounting for short-term wind forecast uncertainty information is not applied in this paper (i.e., perfect forecasting of the wind power time series is assumed), though could be included if desired—unit commitment methods that account for such forecast uncertainty by producing flexible conventional plant schedules have been reported in [18] and [19]. Stochastic scheduling tools are very computationally expensive however. At lower levels of wind penetration, operational timeframe wind forecast uncertainty may have little effect on long-term power transmission planning problems. Longer-term uncertainty relating to input parameters such as fuel or carbon price, peak customer load etc., can be reflected in alternative scenarios.

3) Formulating the Load Flow Inequality Constraints: The "dc" load-flow [6] uses the transmission line reactance values to determine a set of linear coefficients α_{ij} [or "power transfer distribution factors" (PTDFs)] that along with a designated power flow reference bus r, define the power flow solution f_j in each branch j as a linear combination of the power injections P_i at every other bus i, as in (3). An important advantage of dc load-flow is that linear constraints can be formulated to represent network power flow security criteria at the LP optimization stage—as will be seen in Section II-B4, this advantage is critical to reducing the LP wind capacity optimization subproblem dimensionality to a manageable size:

$$f_j = \sum_{i \neq r} \alpha_{ij} \times P_i. \tag{3}$$

The dc load flow is often used in planning studies as a very good approximation to the transmission network's active power transport requirement. Other important network operational characteristics such as steady-state and dynamic voltage behavior, short-circuit levels as well as transient stability are more suited to detailed in-depth analysis [20], may not be fully amenable to a manageable optimization process across such a range of power flow conditions, and are typically assessed once the grid is known to be thermally secure. The algorithm outlined in this paper can be viewed as an optimistic total wind capacity allocation from which to carry out such analyses, with due consideration of advanced technology solutions [21]. If desired, spare line capacity can be set aside for related reactive power flows or known system stability constraints. Fine-tuning of assumed thermal line capacity limits can be carried out in each hour with updated information from subsequent system dynamic and full ac load flow studies—this may be necessary as wind generators, specifically squirrel-cage induction machines, can have a high reactive power demand. On the other hand, studies have shown that the addition of wind capacity to a network can improve the voltage profile in some areas if controlled reactive power output is applied using wind turbine power electronics [10], [22].

Assessing power system capability with respect to traditional security criteria across the entire time-length of the time series study implies a very large number of power flow scenarios. In the limit this value is defined by (4), for T years of hourly data analysis, considering each contingency at each hour of the year with respect to each other line's capacity (any single generator (G) and/or simultaneous single network branch (N) contingency state is modeled in this paper):

$$T \times 8760 \times N \times (N-1) \times G. \tag{4}$$

The localized impact of any possible branch contingency would suggest that not all such contingency scenarios realistically need to be modeled. Comparing the probability density functions of the initial system's yearly load flows in each line under intact-network and each other branch-outage condition can be used as a heuristic contingency screening method—load flow

probability density functions with wide spreads and the most extreme maximum values correspond to the most onerous contingency cases for that line. An initial visual check of these load flow spreads can be carried out to select the network configurations of relevance for subsequent study. Alternatively, network contingency selection could be carried out in a more automated manner on the basis of the network's "line-outage distribution factors" [6]. For each generation contingency, an appropriate reserve response is allocated from the reserve dispatch of step 2 (Section II-B2) in each hour so that load balance is maintained. In all, a combined total of S network power injection (i.e., each intact and post-generation-contingency MW power dispatch) and network branch (i.e., each set of PTDFs for the intact network and relevant line outage states) contingencies are applied to each hour of the time series.

As the principle of superposition applies to linear dc load flow, the power flow contribution from both load and conventional generation can be evaluated as numerical partial load flow solution value γ_{jhs} for each hourly security scenario using the relevant MW dispatch information (step 2) and the dc load flow coefficients. The collective net contribution of the k wind farms to the power flows as superimposed values in each of S hourly intact/contingency system configurations is as of yet unknown. The wind capacity allocation optimization variables C_k when scaled by their respective nominal 1-MW hourly time series values t_{kh} and the relevant dc load flow coefficients will determine this. The inequality constraints of (5) are thus included for each of S system configurations in each hour h to ensure that the wind capacity allocations do not overload any of the network thermal line capacities L_j, in either the forward or backward flow directions. The optimized firm wind capacity related power flows are essentially "fitted-around" the existing firm conventional plant production power flows from Section II-B2, ensuring both network security and power system balance under each critical contingency. The double-sided inequalities of (5) can be represented as single-sided inequalities by the algebraic manipulation of (6), (7). Each wind plant's capacity is modeled as a continuous optimization variable, as individual turbine size is relatively small in comparison. The turbine capacity optimization variables will of course be non-negative, as specified by (8). Wind plant contingencies can be modeled by assuming their wind power time series t_{kh} is zero in the hours of interest, but the related primary reserve bus power injection required to replace their power production generation contingency can only be modeled for subsequent re-iterations (Section II-B6) as the individual wind plant capacities are initially unknown:

$$\forall_{h,j,s}\left[-L_j \le \sum_k \alpha_{kj_S} \times t_{k_h} \times C_k + \gamma_{j_{hs}} \le L_j\right] \quad (5)$$

$$\forall_{h,j,s}\left[\sum_k \alpha_{kj_S} \times t_{k_h} \times C_k - (L_j - \gamma_{j_{hs}}) \le 0\right] \quad (6)$$

$$\forall_{h,j,s}\left[\sum_k -\alpha_{kj_S} \times t_{k_h} \times C_k - (L_j + \gamma_{j_{hs}}) \le 0\right] \quad (7)$$

$$\forall_k \qquad C_k \ge 0. \quad (8)$$

4) Removing Redundant Linear Constraints: Optimization algorithm computational requirements are sensitive to both the number of variables and constraints in the mathematical model applied [23]. A refined version of the algorithm introduced in [13] is applied here to reduce the LP model constraint dimensionality. An approximate method of contingency selection before formulation of the hourly line flow constraints was described in Section II-B3. Additional model efficiency can be achieved if redundancy in the inter-hourly behavior of these selected network cases as described by (6) and (7) is also considered. Constraint redundancy will occur when inequality constraints as represented by lines L_2 and L_4 in Fig. 2 do not intersect the optimization feasible space, as defined by the inner convex polygon of inequality constraints L_1, L_3 and the variable axes [note the capacity variables cannot be negative as specified in (8)]. They will thus not influence the solution of any optimization model.

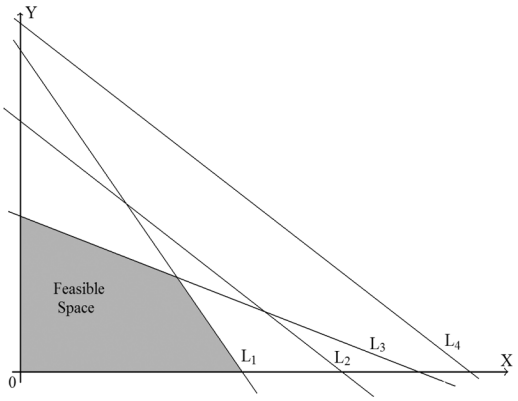

Fig. 2. Linear program constraint redundancy—no feasible space intersection.

Dulá in [24] gives an extensive mathematical treatment of linear programming redundancy, outlining the frame or extreme-point subset of the convex-hull of multidimensional data points representing the dual problem constraint matrix formulation as the source of the non-redundancy in the primal representation. As the convex hull of any general type of multidimensional point dataset can define every point within its multidimensional convex volume, it is the minimal complete representation of the multidimensional dataset [25], and all points interior to the convex hull may be considered redundant. Dulá *et al.* in [26] also describe an efficient computational method to determine the frame of the convex hull of a point dataset by testing the feasibility of successively larger linear programs.

The presence of (8) in the LP optimization constraint set allows an intuitively simpler interpretation of the linear constraint redundancy issue for this paper. Consider two arbitrary linear constraints as in (9a) and (9b) below. As X, Y are ≥ 0 in this problem, then if all the coefficients and constant of (9a) (i.e., a_1, a_2, $const_a$) are at least greater than or equal to their equivalents in (9b), then (9b) (corresponding to line type L_4 in Fig. 2) will intuitively be a less extreme constraint and is thus made redundant by (9a):

$$a_1 \cdot X + a_2 \cdot Y + \ldots + const_a \le 0 \quad (9a)$$

$$b_1 \cdot X + b_2 \cdot Y + \ldots + const_b \le 0. \quad (9b)$$

The geometric dual of a line (and thus a linear programming optimization inequality constraint) is a point [25], and similarly

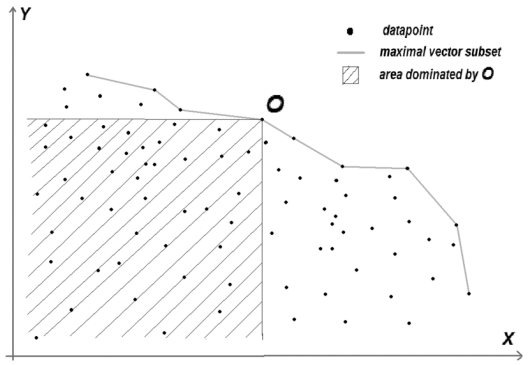

Fig. 3. Maximal vector subset of a 2-D dataset.

each constraint such as (9a) and (9b) can be uniquely represented with the geometric points p_a and p_b—for example

$$p_a \equiv \left(\frac{\mathrm{a}_1}{|\mathrm{const_a}|}, \frac{\mathrm{a}_2}{|\mathrm{const_a}|}, \frac{\mathrm{const_a}}{|\mathrm{const_a}|}\right) \equiv (\omega_{a1}, \omega_{a2}, \omega_{a3}) \tag{10a}$$

$$p_b \equiv \left(\frac{\mathrm{b}_1}{|\mathrm{const_b}|}, \frac{\mathrm{b}_2}{|\mathrm{const_b}|}, \frac{\mathrm{const_b}}{|\mathrm{const_b}|}\right) \equiv (\omega_{b1}, \omega_{b2}, \omega_{b3}). \tag{10b}$$

As outlined by the authors in [13], the complete set of inequality constraints in (6) and (7) can therefore be equally defined in this simple manner as a very large cardinality multi-dimensional point dataset. The problem of quickly removing many redundant linear inequality constraints in this LP optimization model is analogous to finding points that do not form the "*maximal vector*" subset of the geometric point dataset—see the "floating currency" analogy to (9a) and (9b) in [27]. A data-point is a maximal vector of a point dataset if it is not dominated by any other data-point—this concept was first introduced in [27] and [28]. p_a dominates p_b if $\omega_{b1} < \omega_{a1}$, and $\omega_{b2} < \omega_{a2}$, and $\omega_{b3} < \omega_{a3}$, etc. Other computational geometry problems such as the "Pareto set" problem and the "skyline" problem [29] have direct correspondence to the maximal vector problem. The maximal vector subset of an arbitrary two-dimensional point dataset is graphically illustrated in Fig. 3. The shaded area in Fig. 3 corresponds to the area containing points dominated by maximal vector point O.

Maximal vectors with individual point co-ordinate values that are all greater than average for that dimension will tend to dominate many other points. Instead of a purely naïve sequential search and comparison, a much more efficient redundancy assessment should therefore incorporate an intelligent preprocessing scheme. Godfrey *et al.* in [30] discussed a data vector coefficient entropy sum to order an arbitrary dataset of points prior to the maximal-vector search and comparison process. If data-points that correspond to very dominant maximal vectors are cycled through the dataset first, they will remove proportionally a much greater than average number of redundant data points, and an efficient redundancy removal process will result. The M data-points still present at the end of the comparison scheme correspond to the dominant maximal vector subset. The discarded or dominated points correspond back to redundant constraints in the LP optimization model (e.g., line L_4 in Fig. 2) [13]. However, within the set of M remaining maximal vector points there may remain a small number of constraints of the type L_2 in Fig. 2—i.e., those that do not define the feasible space yet are not fully dominated by any other single constraint. This is not critical, as the objective of the LP preprocessing stage is to remove a lot of redundant constraints quickly, rather than to fully identify the minimum set of constraints defining the LP feasible space—refer to [24] and [26] for such an algorithm.

As in [13] this paper uses the product of the "rank" of each point coordinate ω_d (i.e., its ordered hierarchical position with respect to the other constraint coefficients for that optimization variable, a term unrelated to linear algebra matrix rank) to determine the ordered position of the data-point p at the search and comparison stage as defined in (11). This is a particularly efficient preprocessing scheme as coefficient ranks are naturally a good measure of each data-point's dominance in the overall dataset. Redundancy removal progress will slow down as data-points with lower overall coefficient rank product are tested for maximal vector dominance. However the total time to carry out the LP optimization stage is the sum of the preprocessing and optimization solver times, so it is wise to implement a stopping criterion, i.e., when the remaining number of constraints is less than a defined number V, which is well within the capabilities of the optimization solver in use:

$$order\,[p(\omega_1, \omega_2, \ldots \omega_{k+1})] \propto \prod_{d=1}^{k+1} rank[\omega_d]. \tag{11}$$

5) Linear Programming Firm Wind Energy Feasibility Test: A linear programming model can be applied to the wind capacity optimization model feasibility test for each incremental wind energy penetration target δ, as all of the constraints are linear in nature and the simple linear cost function of (12) was applied here. The outputs of this single-stage LP model are the collectively optimized firm wind capacities that ensure the feasibility of this wind energy penetration level (i.e. so that the wind energy target is achieved and that no network branches are overloaded pre- or post-contingency during the extended time-period of investigation), while minimizing the chosen cost function. In theory, the feasibility of each $\Delta\delta$ firm wind energy connection target is determined by the linear constraints alone and should not be sensitive to the cost function applied. The cost function choice may affect the convergence of the overall methodology solution and individual allocations of wind capacity however.

The energy contribution of a wind farm is defined by its capacity factor value. The LP wind capacity allocation must satisfy the total system wind energy penetration δ assumed in the scheduling stage of Section II-B2. This is ensured with the inclusion of (13), where λ_k is each wind farm's capacity factor, and the respective wind capacity allocations C_k are the optimization variables. For the given firm wind energy connection target, the constraint of (8), as well as the V remaining network power flow inequality constraints set of (14) and (15) [originally a subset of (6) and (7)] will also apply. The complete linear programming model is summarized by (8), (12), (13), (14), and (15):

$$Cost = Min\left(\sum_k C_k\right) \tag{12}$$

$$\sum_k C_k \cdot \lambda_k = D^{AVG} \cdot \delta \tag{13}$$

$$\forall_{v\in V}\left[\sum_{k}\alpha_{kj_v}\times t_{k_v}\times C_k-(L_j-\gamma_{j_v})\le 0\right] \quad (14)$$

$$\forall_{v\in V}\left[\sum_{k}-\alpha_{kj_v}\times t_{k_v}\times C_k-(L_j+\gamma_{j_v})\le 0\right]. \quad (15)$$

6) Updating the System-Total Wind Power Time Series: The formulation of the MIP unit-commitment/dispatch problem in Section II-B2 used an approximate geographically-smoothened total wind power output time series. This may not necessarily correspond precisely to the total wind power time series resulting from the LP output wind turbine capacities when scaled by their individual nominal 1-MW wind power time series. In order to preserve power system balance at each operational hour, steps 2, 3, 4, and 5 of the methodology can be reiterated (within each wind penetration target level δ) using the new total wind power time series resulting from the LP model of the last iteration. The LP output wind turbine capacities may change slightly from one re-iteration to the next; however after a few iterations the total wind power output time series resulting from the LP model converges to that used as input to the unit-commitment/dispatch subtask, and the turbine capacities from the LP model will subsequently remain unchanged. This re-iteration ensures consistency between the separated MIP unit-commitment/dispatch and the LP wind capacity allocation subtasks.

7) Incrementing the Firm Wind Energy Penetration Target: Estimating the maximum possible wind energy integration using firm wind capacity can be approached as a series of simpler LP model feasibility tests—by increasing the wind energy target δ in small discrete increments of $\Delta\delta$, steps 2, 3, 4, 5, and 6 of the methodology are repeated until a feasible solution to the LP model of Section II-B5 using firm wind capacity allocation to distinct transmission buses no longer exists. The methodology outlined in this paper is separated into smaller optimization subproblem steps, as illustrated in Fig. 1. This ensures the ability to separate the MIP system scheduling and large-scale LP wind capacity placement tasks and ensure a practical computational implementation (by exploiting the linear constraint redundancy as detailed in Section II-B5). While this overall methodology will improve firm wind energy connection feasibility, given the inclusion of MIP variables and the practical separation of the individual subtasks of the optimization problem, it is unlikely that the absolute global optimal solution can be found however, nor any measure defined with regard to how far the proposed solution is from global optimality.

III. Methodology Application to a Test-System

The test network used for the illustration of this firm wind energy connection maximization methodology was a simple 35-bus, 54-line model as depicted in Fig. 4 (with network parameters based on a subset of the Irish "All-Island" 220/275/400-KV high voltage transmission system). Historical synchronously recorded wind power output data of one year's length, load time series data, and a subset of the existing conventional plant from the Irish power system were combined with the test network of Fig. 4 for study. The total conventional generation capacity was 2256.1 MW. The assumed peak load for the test system was 1825.2 MW. The average load was

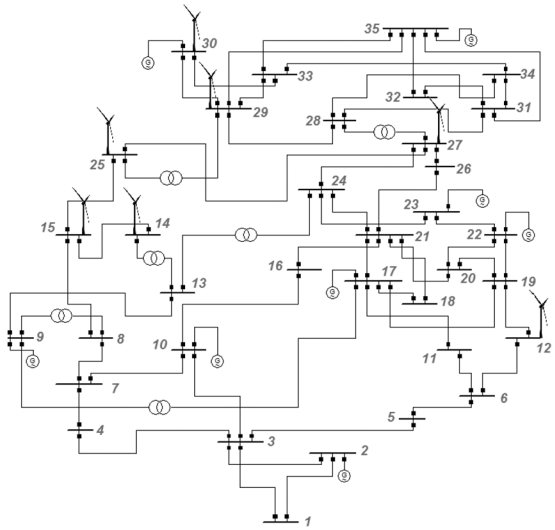

Fig. 4. Test system transmission network schematic.

1246.6 MW. The network branch capacity values chosen were commensurate with the zero wind integration power flow scenarios, while providing some extra capacity for subsequent wind connection. It was assumed that seven potential wind generation sites were available, at buses 12, 14, 15, 25, 27, 29, and 30. The synchronously recorded wind time series from the existing wind farms were normalized to 1-MW capacity for use in this analysis. High wind capacity factor time series were arbitrarily located on bus 15, 14, 27, and 12, while lower capacity factor wind farms are available at bus 30, 29, and 25. The unit commitment/dispatch step was carried out using the deterministic scheduling (perfect wind forecasting assumed) software tool PLEXOS [31] in 24-h segments—conventional plant was dispatched on the basis of energy cost. Further test system details are contained in the Appendix.

IV. Results

A. Maximizing the Firm Wind Energy Penetration Level

An initial firm wind energy penetration target δ of 5% was found to be feasible using the methodology of Sections II-B2, 3, 4, 5, and 6. The energy penetration target was updated in small increments until a 10% target was found to be infeasible. The 9.5% target (i.e., $\delta = 0.095$) was therefore estimated by this decomposed optimization methodology as the maximized firm wind energy penetration level. A table of the collectively optimized firm wind capacity allocations at each wind energy penetration increment is given in Table I.

The firm capacity allocation to the wind farm at bus 15 in successive steps is particularly interesting. As the system wind energy integration target is increased the firm capacity allocation to this node (which has the highest capacity factor) initially increases but then decreases. This illustrates the trade-off between individual wind farm capacity allocation and each farm's contribution to facilitating the maximum possible firm wind energy penetration in the system as a whole. It also underlines the benefit of collectively considering all potential wind farms with the formal optimization model as outlined in Section II.

TABLE I
OPTIMIZED WIND ENERGY PENETRATION CAPACITY ALLOCATIONS (MW)

Energy % Penetration	Wind Farm Bus Number						
	12	14	15	25	27	29	30
5	0	0	93.1	0	81.4	0	0
6	0	0	101.3	0	90.2	0	0
7	0	0	88.1	9.5	147.0	0	0
8	33.4	38.9	45.0	35.5	138.9	0	0
9	73.6	51.6	44.6	30.9	128.3	0	0
9.5	68.7	54.6	51.5	40.2	132.7	0	0
10	*<infeasible>*						

TABLE II
THE 9.5% WIND ENERGY RE-ITERATED WIND CAPACITY ALLOCATIONS (MW)

Iteration Number	Wind Farm Bus Number						
	12	14	15	25	27	29	30
1	63.6	55.7	51.9	42.2	134.3	0	0
2	68.6	52.8	52.8	40.8	132.7	0	0
3	68.7	54.6	51.5	40.2	132.7	0	0

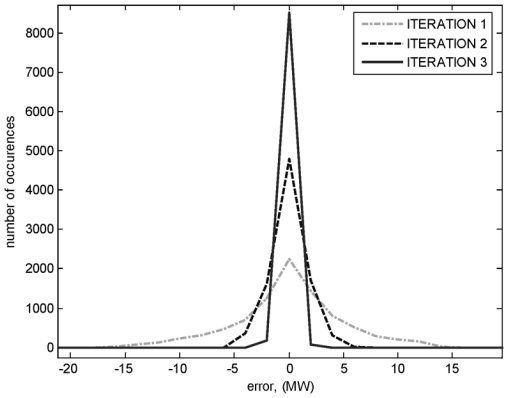

Fig. 5. Histogram of power imbalance between methodology re-iterations.

B. Convergence of the System-Total Wind Power Time Series

As described in Section II-B6, the methodology of Sections II-B2, 3, 4, and 5 was successively repeated using the updated LP model wind capacity allocation results, to remove any load/generation mismatches. Some changes in the integer unit-commitment and linear dispatch variables (e.g., for conventional generators at the margin in each hour) do occur in step 2 from one re-iteration to the next until the solution converges between iterations. A table of the LP optimal capacity allocations at each of the methodology re-iterations for the largest feasible wind energy penetration target (9.5%) is given in Table II below. Histograms of the load/generation mismatch error at each hour between successive re-iterations for this firm wind energy penetration level are also illustrated in Fig. 5. Reiteration of the subtasks from the first iteration results gradually converges to a solution preserving consistency between the assumed input time series for MIP unit commitment/dispatch and the time series determined by the LP wind capacity allocation model output solution (though as discussed in Section II-B7, Fig. 5 does not prove convergence to the global optimum). A similar effect was observed for each of the other wind energy penetration levels.

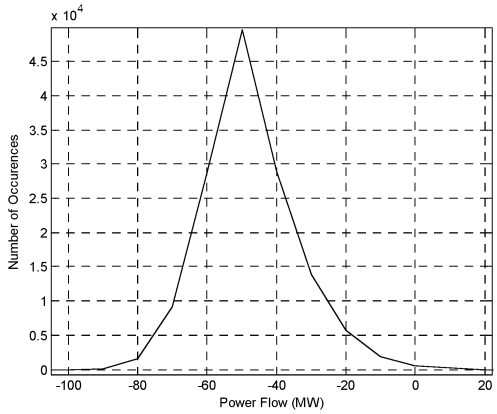

Fig. 6. Load flow distribution for branch 6–12 under branch 11–17 failure.

C. Investigating the Solution Load Flow Results

At the end of the firm wind capacity allocation methodology, the optimized wind farm capacities can be used to carry out the resultant time series load flow to ensure that system security is indeed maintained at each of the individual hours. For completeness, this should include all possible line and generation contingencies from (4), irrespective of both the initial contingency screening of Section II-B3 and the mathematically rigorous constraint redundancy elimination of Section II-B4. The histogram of the year-long power flows in the network branch from bus 6 to bus 12 under all possible single generation contingency events and a single outage contingency in the branch from bus 11 to bus 17 is illustrated in Fig. 6. No cases result in power flow exceeding the thermal line capacity of 100 MW—hence the advantage of the year-long extended timeframe analysis. As the very edge of the line flow distribution corresponds to the branch thermal capacity 100 MW, it is clear that this line is a binding constraint on the firm wind energy connection process.

D. Computational Requirements

The year-long conventional generation scheduling and dispatch task, using a rounded-relaxation solution method in PLEXOS, took approximately 20 min on average for each of the iterations on the test system's generation portfolio, implemented on a 3.6-GHz Pentium dual-core driven, 4 GB of RAM enabled Dell Optiplex GX620 desktop PC. Considering the initial LP problem dimensionality of (4) for the simple test system in Section III would have resulted in $\sim 400 \times 10^6$ line power flow security cases for the entire year of study. The contingency screening technique based on the initial zero-wind time series load flow investigation of Section II-B3 reduced this to $\sim 49.34 \times 10^6$ constraints using a simple visual test—this contingency set was identified and applied to all of the subsequent optimization row iterations in Table I. The MATLAB [32] software environment was used to implement the efficient constraint redundancy preprocessing stage of Section II-B4, trimming the original $\sim 49.34 \times 10^6$ possible line flow constraints to a practical user-defined stopping criterion V of 2.5×10^5 in approximately 14 min (on average) for each of the iterations. Scaling of the constraint coefficients by the magnitude of the constant terms [as in (10a) and (10b)] was found to refine the computational time efficiency of this paper's investigation by

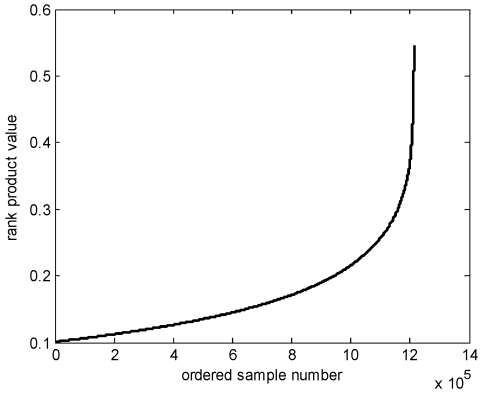

Fig. 7. Typical graph of ordered rank-product values for preprocessing.

$\sim$40% with respect to the original approach in [13]. The benefit of a preprocessing stopping criterion was also investigated. At the 3rd iteration of the final feasible 9.5% wind energy penetration, when the constraint redundancy analysis was allowed to generate the absolute minimal cardinality set of M non-dominated maximal vectors, only 6.823×10^3 constraints remained, though the computational time trade-off of 149.37 min was substantial. The LP optimization solver employed was the MATLAB LINPROG medium-scale interior-point algorithm. This determined an optimized solution to the reduced LP problem of Section II-B5 (with 2.5×10^5 constraints) in approximately 3.14 s (the minimal set of 6.823×10^3 constraints was solved in 0.47 s in comparison). Post-optimal processing indicated that only four of the line flow constraints were binding on the output solution for the 9.5% firm wind energy connection level, i.e., four of the lines' maximum flow values reached their defined capacity levels at some stage over the year of analysis. A typical graph of the increasing order of constraint rank-product values from (11) can be seen in Fig. 7. As Fig. 7 illustrates, the sparsity of extreme constraints in the firm wind capacity power system planning problem investigated here suggests that relatively few constraints will dominate most of the others, underlining the benefit of applying the ordered maximal-vector redundancy preprocessing step of Section II-B4.

V. Discussion

A methodology to estimate the maximum firm wind energy that can be integrated to a given power transmission network is outlined in this paper. Wind fluctuations and statistical dependence have been explicitly accounted for through the use of multivariate year-long historical recorded time series. This paper applied fixed contingency security criteria for each of the hours of the yearly duration time series. This generated a very large dimensionality system power flow model. A decomposition of the firm capacity allocation problem into separate MIP unit-commitment/dispatch and LP wind capacity placement steps using a geographical-smoothing approximation of system-total wind power output allowed the design of a preprocessing algorithm to exploit the overwhelming redundancy in the structure of the associated LP model subtask. Decomposing the overall firm capacity optimization problem into separate subtasks reduces the problem complexity and allows a practical implementation with standard computing resources to achieve improved feasible firm wind energy integration solutions. An associated difficulty however is the inability to guarantee global optimality or determine the solution optimality gap.

Using initial contingency screening combined with an efficient and rigorous maximal-vector based redundancy algorithm, a reduction of the test-system's original constraint dimensionality by $>99.9\%$ (to 2.5×10^5) was possible. Similar computation efficiency should be achievable in larger power systems, with the possible use of parallelized preprocessing. Implementation of the preprocessing algorithm in a faster execution environment than MATLAB could also produce greater efficiency. Commercial optimization solvers such as CPLEX also use some model preprocessing approaches and report that they can handle "millions" of constraints and variables [33]. The linear inequality constraint dimensionality in even a medium-sized power system could stretch to the order of billions however, as suggested by (4), so one would expect some user preprocessing may need to be carried out before attempting a solution. The algorithm of Section II-B4 was tailored specifically for the LP model in this paper, though other linear constraint redundancy removal algorithms have also been proposed previously [26], [34]. While the maximal-vector method in this paper illustrates the overwhelming redundancy present in the LP constraint structure of the applied problem, future work could benchmark its performance against alternative algorithms to evaluate its efficiency. The maximal-vector method is by no means restricted to LP optimization problems in the power systems domain—as long as the conditions of Section II-B4 are satisfied then it should be applicable to other problems.

While the overall goal of the paper is the integration of wind energy, the methodology uses firm wind capacity only to achieve this (i.e., no transmission congestion allowed). While the maximal-vector subset cardinality M of 6.823×10^3 constraints was less than 0.000017% of the total constraint set, a post-optimal analysis of the linear programming steps furthermore indicated that only a handful of these M constraints were actually binding on the solutions obtained. This would suggest that wind plant behavior in a few hours of the year determined the firm wind capacity allocation in the entire system. Given the particularly low capacity credit of wind power, and acknowledging the rarity of such worst-case scenarios with a low capacity factor source of generation such as wind (see the relative spread of the extremities of Fig. 6 and the ordered shape of Fig. 7), the results of this paper suggest it would be more prudent in future study to have the connection of "non-firm" wind capacity (that can economically accept a defined level of energy curtailment over a fixed time period [35]), as the central optimization variables of interest. However that optimization problem complexity is certainly of a non-trivial nature—it would imply a very large scale hourly security-constrained-OPF problem with linear dispatch variables, solved within a daily mixed integer unit-commitment problem, both of which are furthermore coupled to the overall wind capacity investment variables spanning the entire length of the applied time series.

The results of the algorithm application to the test system network in this paper are based on a representative set of multivariate historical wind power time series of 1 year's length (though obviously multiple years of data could be used if available). Wind power output profiles may change from year to

year—using a number of years wind data will improve accuracy and solution robustness. Wind data growing techniques such as those proposed in [36] could also be applied. Any successful wind data growing technique must preserve both the individual wind plant cross-correlative behavior (for accurate load-flow) but also the auto-correlative trends of total system wind power output (for system unit commitment). Diurnal or seasonal influences in wind production patterns should also be accounted for. The nominal 1-MW wind time series required in Section II-B1 are assumed to be independent of the optimized wind capacity solution outputs determined by Section II-B5. This is acceptable in reality as the optimized wind capacity to be allocated to each transmission system bus would likely be the sum of capacities of dispersed (possibly distribution-connected) wind farms in the nearby area, and as the hourly nominal wind time series data described in Section III was scaled from existing large multi-MW wind farms installed on the Irish power system.

A connection queue is typically used in modern deregulated power systems for generation project connection sequencing. The algorithm outlined in this paper attempts to estimate the maximum possible wind energy connection with firm capacity as new transmission projects are implemented. A larger subset of the original firm connection queue projects can be satisfied, though not necessarily in accordance with their actual position in the queue. It may therefore seem more related to the composite system planning techniques of the traditional vertically integrated utility. Until significant new transmission capacity is built however, optimal use of networks could be made in the interest of accelerating wind power connection in the short to medium term. Recognising the fundamentally different characteristics of wind energy, a return to some level of integrated planning may be required [37].

VI. Conclusion

This paper presents a methodology with the aim to maximize the firm wind energy penetration to any given power transmission network. Applying security criteria over the extended sequential timeframe required to model wind power variations generates a high-dimensionality optimization model—separation of the MIP unit-commitment/dispatch and LP firm wind capacity placement problems allows a maximal-vector based preprocessing technique to filter out a substantial proportion of constraint redundancy present in the LP model. While solution global optimality is not guaranteed with this approach, a significant advantage is the reduction in model complexity. The optimized capacity results indicate a balance between each wind site's capacity factor (or position in a connection queue), and the overall goal of maximizing the total firm wind capacity connection potential of the power system as a whole, is prudent. Post-optimal analysis underlines the importance of considering wind as a "non-firm" energy source rather than a firm capacity source in future methods—i.e., for currently congested systems where much more wind might be integrated if limited curtailment is acceptable.

Appendix

Tables III–VI list the wind farm time series capacity factors, branch reactance parameters and capacity limits, maximum bus load values, and conventional plant information, respectively, for the test system described in Section III.

TABLE III
Wind Farm Time Series Capacity Factors

Wind Farm Capacity Factor	Wind Farm Bus Number						
	12	14	15	25	27	29	30
	0.33	0.35	0.36	0.29	0.34	0.29	0.31

TABLE IV
Branch Reactance Parameters and Capacity Limits

FROM BUS	TO BUS	X_L (100 MVA BASE)	LIMIT (MW)	FROM BUS	TO BUS	X_L (100 MVA BASE)	LIMIT (MW)
1	2	0.02	400	18	21	0.044	150
1	3	0.02	400	19	20	0.01	160
2	3	0.011	400	19	22	0.01	320
3	4	0.039	250	20	21	0.01	300
3	5	0.075	225	20	22	0.01	320
3	10	0.073	300	21	24	0.02	280
4	7	0.084	200	21	26	0.038	410
5	6	0.02	280	22	23	0.003	370
6	11	0.06	170	23	24	0.008	370
6	12	0.076	100	24	27	0.053	440
7	8	0.007	400	25	27	0.095	240
7	10	0.061	220	25	29	0.025	450
8	9	0.042	380	26	27	0.03	330
8	15	0.077	270	27	28	0.025	440
9	13	0.023	430	28	29	0.011	180
9	17	0.079	350	28	31	0.0185	150
10	16	0.08	175	28	34	0.036	100
11	17	0.051	175	29	30	0.011	230
12	19	0.046	175	29	33	0.0135	130
13	14	0.04	250	29	35	0.0282	100
13	24	0.046	380	30	33	0.02	330
14	15	0.029	240	31	32	0.005	110
15	25	0.076	285	31	34	0.0294	110
16	21	0.094	220	31	35	0.02	130
17	18	0.022	160	32	35	0.0196	130
17	19	0.036	210	33	34	0.0065	90
17	21	0.016	330	33	35	0.0198	100

TABLE V
Maximum Bus Load Values

Bus	Load (MW)	Bus	Load (MW)
1	59.37	19	117.86
2	2.62	20	117.28
3	75.96	21	77.41
4	20.66	22	191.784
5	74.5	23	20.37
6	9.57	24	0
7	37.25	25	82.07
8	0	26	75.96
9	25.03	27	74.21
10	64.32	28	98.95
11	29.48	29	34.92
12	48.89	30	86.72
13	5.093	31	75.37
14	0	32	58.20
15	91.09	33	42.20
16	63.73	34	0
17	17.46	35	46.86
18	0		

TABLE VI
CONVENTIONAL PLANT INFORMATION

Bus Number	Plant Description	
	Capacity (MW)	Fuel
2	3*95	Gas (OCGT)
9	2*286	Coal
10	1*83	CHP
17	1* 90, 1*117.6	Peat
22	3*109.5	Oil
23	1*400	Gas (CCGT)
30	2*95	Gas (OCGT)
35	2*95	Gas (OCGT)

ACKNOWLEDGMENT

The authors thank Mr. P. Smith, Mr. M. Burke, Mr. M. Norton, Dr. J. O'Sullivan and others from the Irish TSO Eirgrid, for their insights and timely cooperation in the supply of data.

REFERENCES

[1] Delivering Energy and Climate Solutions—EWEA 2007 Annual Report, European Wind Energy Association (EWEA), Mar. 2008. [Online]. Available: http://www.ewea.org/index.php?id=178.
[2] 20% Wind Energy by 2030—Increasing Wind Energy's Contribution to U.S. Electricity Supply, U.S. Department of Energy, May 2008.
[3] All Island Grid Study, Workstream 4—Analysis of Impacts and Benefits, Irish Government Department of Communications, Energy and Natural Resources/United Kingdom Department of Enterprise, Trade and Investment, Jan. 2008. [Online]. Available: http://www.dcenr.gov.ie/Energy/North-South+Co-operation+in+the+Energy+Sector/All+Island+Grid+Study.htm.
[4] A Study on the Comparative Merits of Overhead Electricity Transmission Lines Versus Underground Cables, Ecofys. [Online]. Available: http://www.dcenr.gov.ie/Energy/Independent+Study+on+Electricity+Transmission+Infrastructure.htm.
[5] R. Moreno, C. V. Konstantinidis, D. Pudjianto, and G. Strbac, "The new transmission arrangements in the UK," presented at the IEEE PES General Meeting, Calgary, AB, Canada, Jul. 2009.
[6] A. J. Wood and B. F. Wollenberg, *Power Generation, Operation and Control*, 2nd ed. New York: Wiley, 1984.
[7] Transmission Forecast Statement 2007–2013, Eirgrid, Aug. 2007. [Online]. Available: http://www.eirgrid.ie/EirgridPortal/.
[8] P. Zhang and S. T. Lee, "Probabilistic load flow computation using the method of combined cumulants and Gram-Charlier expansion," *IEEE Trans. Power Syst.*, vol. 19, no. 1, pp. 676–682, Feb. 2004.
[9] C. L. Su, "Probabilistic load-flow computation using point estimate method," *IEEE Trans. Power Syst.*, vol. 20, no. 4, pp. 1843–1851, Nov. 2005.
[10] G. Papaefthymiou, "Integration of stochastic generation in power systems," Ph.D. dissertation, TU Delft, Delft, The Netherlands, 2007.
[11] G. Papaefthymiou and D. Kurowicka, "Using copulas for modeling stochastic dependence in power system uncertainty analysis," *IEEE Trans. Power Syst.*, vol. 24, no. 1, pp. 40–49, Feb. 2009.
[12] D. Burke and M. J. O'Malley, "Optimal wind power location on transmission systems—A probabilistic approach," presented at the IEEE PMAPS Conf., Mayaguez, PR, May 2008.
[13] D. Burke and M. J. O'Malley, "Optimal firm wind capacity allocation to power systems with security constraints," presented at the IEEE PSCE Conf., Seattle, WA, March 2009.
[14] J. E. Jackson, *A Users Guide to Principal Component Analysis*. New York: Wiley, 1991.
[15] A. Hyvarinen, J. Karhunen, and E. Oja, *Independent Component Analysis*. New York: Wiley, 2001.
[16] *Wind Power in Power Systems*, T. Ackermann, Ed. New York: Wiley, 2005.
[17] M. Hu, J. Kehler, and D. McCrank, "Integration of wind power into Alberta's electric system and market operation," presented at the IEEE PES General Meeting, Pittsburgh, PA, Jul. 2008.
[18] C. Weber, P. Meibom, R. Barth, and H. Brand, "WILMAR: A stochastic programming tool to analyze the large-scale integration of wind energy," in *Optimization in the Energy Industry*. Berlin, Germany: Springer, 2009, ch. 19, pp. 437–458.
[19] A. Tuohy, P. Meibom, E. Denny, and M. J. O'Malley, "Unit commitment for systems with significant wind penetration," *IEEE Trans. Power Syst.*, vol. 24, no. 2, pp. 592–601, May 2009.
[20] C. W. Taylor, *Power System Voltage Stability—International Edition*. Singapore: McGraw-Hill, 1994.
[21] D. Sullivan, M. Takeda, A. Johnson, J. Paserba, S. Yasuda, and R. Tucker *et al.*, "Dynamic voltage support with the rector SVC in California's San Joaquin Valley," presented at the IEEE T&D Conf. Expo., Chicago, IL, Apr. 2008.
[22] E. Vittal, A. Keane, and M. J. O'Malley, "Varying penetration ratios of wind turbine technologies for voltage and frequency stability," presented at the IEEE PES General Meeting, Pittsburgh, PA, Jul. 2008.
[23] P. Gill, W. Murray, and M. Wright, *Practical Optimization*. London, U.K.: Academic, 1981.
[24] J. H. Dula, "Geometry of optimal value functions with applications to redundancy in linear programming," *J. Optim. Theory Appl.*, vol. 81, no. 1, pp. 35–52, Apr. 1994.
[25] M. DeBerg, M. Van Kreveld, M. Overmars, and O. Schwarzkopf, *Computational Geometry Algorithms and Applications*, 2nd ed. Berlin, Germany: Springer-Verlag, 2000.
[26] J. H. Dula and R. V. Helgason, "A new procedure for identifying the frame of the convex hull of a finite collection of points in multidimensional space," *Eur. J. Oper. Res.*, vol. 92, pp. 352–367, 1996.
[27] F. P. Preparata and M. I. Shamos, *Computational Geometry—An Introduction*. New York: Springer-Verlag, 1985.
[28] H. T. Kung, F. Luccio, and F. P. Preparata, "On finding the maxima of a set of vectors," *J. ACM*, vol. 22, no. 4, pp. 469–476, Oct. 1975.
[29] D. Kossman, F. Ramsak, and S. Rost, "Shooting stars in the sky—An online algorithm for skyline queries," in *Proc. 28th VLDB Conf.*, Hong Kong, 2002.
[30] P. Godfrey, R. Shipley, and J. Gryz, "Maximal vector computation in large data sets," in *Proc. 31st VLDB Conf.*, Trondheim, Norway, 2005.
[31] Energy Exemplar. [Online]. Available: http://www.energyexemplar.com.
[32] The Mathworks. [Online]. Available: http://www.mathworks.com/.
[33] ILOG CPLEX. [Online]. Available: http://www.ilog.com/.
[34] S. Paulrag, C. Chellappan, and T. R. Natesan, "A heuristic approach for identification of redundant constraints in linear programming models," *Int. J. Comput. Math.*, vol. 83, no. 8–9, pp. 675–683, Aug.–Sep. 2006.
[35] J. Kabouris and C. D. Vournas, "Application of interruptible contracts to increase wind power penetration in congested areas," *IEEE Trans. Power Syst.*, vol. 19, no. 3, pp. 1642–1649, Aug. 2004.
[36] B. Klockl, "Multivariate time series models applied to the assessment of energy storage in power systems," presented at the IEEE PMAPS Conf., Mayaguez, PR, May 2008.
[37] S. T. Lee, "For the good of the whole," *IEEE Power and Energy Mag.*, vol. 5, no. 5, pp. 24–35, Sep./Oct. 2007.

Daniel J. Burke (GS'07) received the B.E.E.E. degree in electrical and electronic engineering from University College Cork, Cork, Ireland, in 2006. He is currently pursuing the Ph.D. degree in power systems at the Electricity Research Centre in University College Dublin, Dublin, Ireland.

Mark J. O'Malley (F'07) received the B.E. and Ph.D. degrees from University College Dublin, Dublin, Ireland, in 1983 and 1987, respectively.

He is a Professor of electrical engineering in University College Dublin and is Director of the Electricity Research Centre with research interests in power systems, grid integration of renewable energy, control theory, and biomedical engineering.